Accurate and simple digital volume correlation using pre-interpolation

Chengsheng Li,[a,b,*] **Rongjun Shu,**[a,b]
[a]State Key Laboratory of Geomechanics and Geotechnical Engineering, Institute of Rock and Soil Mechanics, Chinese Academy of Sciences, Wuhan, Hubei 430071, China
[b]University of Chinese Academy of Sciences, Beijing 100049, China
DOI:10.5281/zenodo.3600641

Abstract. Existing incremental digital volume correlation methods can reduce the number of errors introduced by interpolation calculations in the inverse-compositional Gauss-Newton algorithm (IC-GN) iteration. However, the accuracy of these existing methods is insufficient for some conditions as the curve-fitting method has high computational efficiency but lacks accuracy. A simple pre-interpolation method is proposed to improve the accuracy and computational efficiency of digital volume correlation. First, the pretreatment of a deformed volume image is calculated by the cubic spline interpolation method with the most often chosen interpolation step of 1/2 sub-voxel. Next, the pre-interpolation is calculated only once and the block calculation techniques solve the memory problem. Then, the reference sub-volume in the updated reference volume image is translated into the nearest half-integer voxel position instead of the integer voxel position or other sub-voxel positions. The pre-interpolation method is applied to both the IC-GN and the curve-fitting method. Experimental results show that the maximum mean bias error and the maximum standard deviation of the improved IC-GN are reduced by 34% and 75%, respectively. The improved curve-fitting has better accuracy and computational efficiency than IC-GN under small strain and the curve-fitting method can achieve about 3.2 times speedup than IC-GN.

Keywords: digital volume correlation, pre-interpolation, nearest sub-volume offset.

*Chengsheng Li, E-mail: lichengsheng@outlook.com.

1 Introduction

The Digital Volume Correlation Method (DVC) was developed from mature two-dimensional digital image correlation (DIC) technologies by Bay et al.[1] Since 1999, the DVC algorithm has been widely used to quantify the deformation field of materials under external loading.[2] DVC can contribute to not only a better understanding of the mechanical behavior of materials from the perspective of a microstructural study[3] but also to the verification of the results of 3D finite element simulation.[4] In the past 20 years, many researchers have been committed to improving the accuracy and computational efficiency of DVC algorithms.[5-9] The inverse-compositional Gauss-Newton algorithm (IC-GN) algorithm is an advanced matching algorithm[10] that can accurately estimate displacement fields when large deformation occurs. Although the Hessian matrix only needs to be calculated once in this method, its iterative calculation is still time-consuming. Therefore, Pan et al.[6] used the interpolation coefficient lookup table approach to reduce the amount of calculation, when using the IC-GN algorithm, in order to improve the computational efficiency; they obtained improvement in computational speed but the approach is memory-consuming. The fast Fourier transform algorithm was also introduced into the DVC algorithm for cases of small deformation to improve computational efficiency.[7] In recent years, with the rapid development of GPU hardware and software, GPUs have been gradually employed to accelerate the DVC algorithm and the computational speed was significantly improved compared to that of a CPU.[11] A simple and effective incremental DVC method was proposed by Wang et al.[8] to reduce redundant interpolation calculations and errors introduced by interpolation calculations in IC-GN iterations. The deformation of different regions in a real material was calculated by Wang et al.[9] using the self-adaptive DVC approach; the large deformation is calculated using a small sub-volume size while the small deformation is calculated using a large sub-volume size.

However, there is still space for improvement in the accuracy and computational efficiency of these algorithms. For example, incremental algorithms performing well in terms of computational speed may have problems with accuracy and system stability. The self-adaptive DVC approach has the disadvantage of programming complexity. The accuracy and stability of the curve-fitting algorithm are relatively poor compared to the IC-GN algorithm; however, its computational efficiency is outstanding.[12] The curve-fitting algorithm would still be a good choice if its accuracy could be improved.

In this work, a simple and effective pre-interpolation method is proposed for the DVC algorithm. First, a 1/2 sub-voxel interpolation calculation is performed in advance, using the proposed pre-interpolation method, on a deformed volume image matrix. Then, the sub-voxel displacement is estimated by the DVC incremental algorithm and the curve-fitting algorithm. The pre-interpolation calculation only needs to be carried out once, which reduces the error caused by intensity interpolation of renewed reference correlation points. Finally, the efficiency and capability of the proposed improved DVC approach is demonstrated in practical applications.

2 In-advance interpolation method

2.1 IC-GN—large strain

Interpolation calculation is a time-consuming task in DVC calculations; it significantly influences the computational speed. As mentioned earlier, Pan et al.[6] effectively reduced redundant calculations by using the interpolation coefficient lookup table approach to perform sub-voxel interpolation; however, the deformed sub-volume must be recalculated in each iteration. Subsequently, incremental deformation was employed by Wang et al.[8] to solve the interpolation problem wherein each incremental position of the deformation is mapped to the nearest integer point. Their simulation results show that the calculation efficiency is increased by approximately 2.5 times the initial value and the error caused by intensity interpolation of renewed reference correlation points is reduced. However, according to the results of this algorithm, in cases such as a sub-voxel displacement calculation, the random errors cannot be ignored when the sub-voxel displacement is about 0.5 voxels (assuming a sub-volume size of 41×41×41 the mean bias error is 0.003). Moreover, the systematic error of the incremental algorithm cannot be ignored when the sub-voxel displacement is about 0.25 voxels or 0.75 voxels (assume a sub-volume size is 41×41×41, stand deviation error is 0.007). The accuracy of the incremental algorithm is far lower than that of the normal IC-GN algorithm in some cases. In this study, the combination of the pre-interpolation method and the incremental algorithm is proposed in order to solve these problems.

A basic 3D IC-GN algorithm flowchart is illustrated in Fig. 1. For each measurement point, the robust zero-mean normalized sum of squared difference criterion can be optimized through the sub-voxel displacement determined by the IC-GN algorithm. It can be seen from Eq. (1) that the deformation submatrix needs to be constantly updated in each iteration; the corresponding mathematical operation is the interpolation calculation (more details regarding the DVC algorithm can be found in Ref. 6).

$$C_{ZNSSD}(\Delta\mathbf{p})=\sum_{\xi}\left\{\frac{f(\mathbf{x}+\mathbf{W}(\xi;\Delta\mathbf{p}))-f_m}{\sqrt{\sum_{\xi}[f(\mathbf{x}+\mathbf{W}(\xi;\Delta\mathbf{p}))-f_m]^2}}-\frac{g(\mathbf{x}+\mathbf{W}(\xi;\mathbf{p}))-g_m}{\sqrt{\sum_{\xi}[g(\mathbf{x}+\mathbf{W}(\xi;\mathbf{p}))-g_m]^2}}\right\}^2 \tag{1}$$

where $f(\mathbf{x})$ and $g(\mathbf{x})$ are the gray intensity values at point $\mathbf{x}=(x,y,z)^{\mathrm{T}}$ in the reference and target sub-volumes; $\xi=(\Delta x,\Delta y,\Delta z)^{\mathrm{T}}$ is the local coordinates of integer voxel points in the reference sub-volume; f_m and g_m represent the mean intensity values of reference and deformed sub-volumes; $\mathbf{p}$ is the linear deformation vector; $\mathbf{W}(\xi;\mathbf{p})$ is the linear displacement mapping function used to describe the deformation of the target sub-volume; $\Delta\mathbf{p}$ is the incremental deformation vector; $\mathbf{W}(\xi;\Delta\mathbf{p})$ is the incremental mapping function exerted on the reference sub-volume.

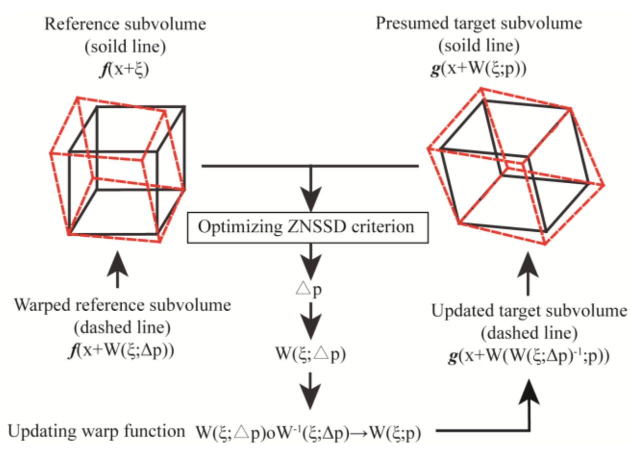

Fig. 1. Schematic illustration of the principle of the 3D IC-GN algorithm.

Since the general CT volume image matrix exceeds 1000×1000×1000 voxels and reduces the memory requirement, the pre-interpolation is usually set to 1/2 sub-voxel interpolation. In this work, the interpolation coefficient α is employed to represent the number of interpolation segments between two points; α is a positive integer. In Figs. 2(a) and (b), the pre-interpolation calculation when $\alpha = 2$ is briefly explained. For example, as shown in Figs. 2(a) and (b), when taking a matrix with 2×2×2 voxel size in the deformed volume image and performing cubic spline interpolation, 19 interpolation points are added at the 1/2 grid nodes. Then, the 2×2×2 voxels matrix is converted into a 3×3×3 voxels matrix and the number of nodes changes from 8 to 27.

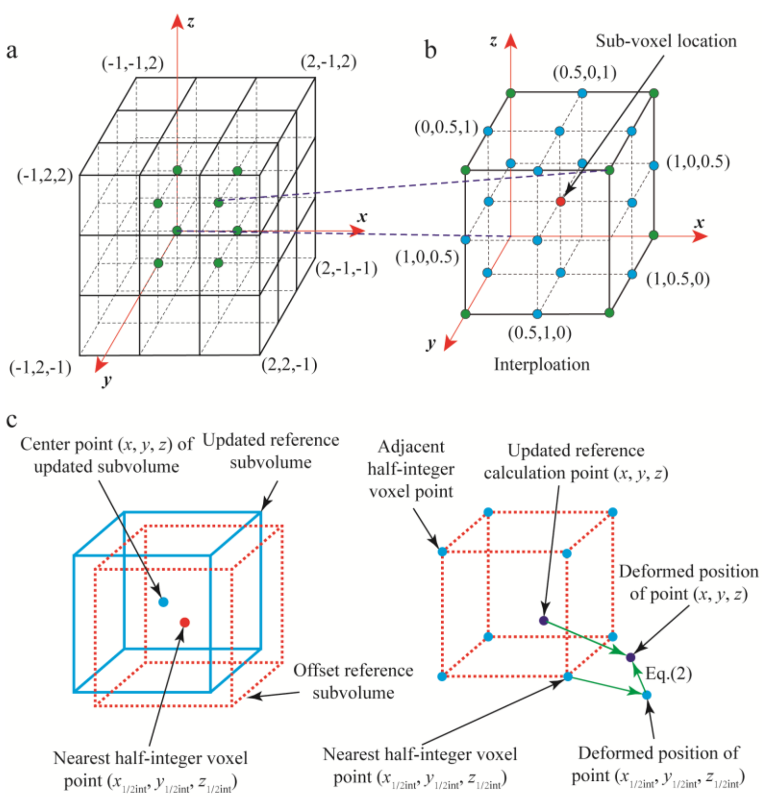

Fig. 2. Schematic illustration of the implementation of cubic spline interpolation with $\alpha = 2$: (a) local interpolation unit comprised of 4×4×4 voxels; (b) interpolation block surrounded by 8 integer voxel points (blue) and 19 half-integer voxel points (green); and (c) schematic of the nearest sub-volume offset approach for incremental DVC.

The interpolated deformation matrix is 2^3-1=7 times larger than the original matrix when α = 2. Although it needs to occupy a massive amount of memory, this problem can be overcome using block calculation techniques (as shown in Fig. 3). According to the memory of a computer, the original matrix can be partitioned in different blocks. s is the maximum displacement, M is the sub-volume size, and the deformed block volume image is bigger than the reference block volume image.

A schematic illustrating the brief flow of the DVC increment algorithm when α = 2 is shown in Fig. 2(c). According to the 1^{st}-order shape function, the incremental displacement vector of the updated measurement point can be estimated by:[8]

$$\begin{bmatrix} u(x,y,z) \\ v(x,y,z) \\ w(x,y,z) \end{bmatrix} = \begin{bmatrix} u(x_{1/2\mathrm{int}}, y_{1/2\mathrm{int}}, z_{1/2\mathrm{int}}) \\ v(x_{1/2\mathrm{int}}, y_{1/2\mathrm{int}}, z_{1/2\mathrm{int}}) \\ w(x_{1/2\mathrm{int}}, y_{1/2\mathrm{int}}, z_{1/2\mathrm{int}}) \end{bmatrix} + \begin{bmatrix} u_x(x_{1/2\mathrm{int}}, y_{1/2\mathrm{int}}, z_{1/2\mathrm{int}}) & u_y(x_{1/2\mathrm{int}}, y_{1/2\mathrm{int}}, z_{1/2\mathrm{int}}) & u_z(x_{1/2\mathrm{int}}, y_{1/2\mathrm{int}}, z_{1/2\mathrm{int}}) \\ v_x(x_{1/2\mathrm{int}}, y_{1/2\mathrm{int}}, z_{1/2\mathrm{int}}) & v_y(x_{1/2\mathrm{int}}, y_{1/2\mathrm{int}}, z_{1/2\mathrm{int}}) & v_z(x_{1/2\mathrm{int}}, y_{1/2\mathrm{int}}, z_{1/2\mathrm{int}}) \\ w_x(x_{1/2\mathrm{int}}, y_{1/2\mathrm{int}}, z_{1/2\mathrm{int}}) & w_y(x_{1/2\mathrm{int}}, y_{1/2\mathrm{int}}, z_{1/2\mathrm{int}}) & w_z(x_{1/2\mathrm{int}}, y_{1/2\mathrm{int}}, z_{1/2\mathrm{int}}) \end{bmatrix} \cdot \begin{bmatrix} (x - x_{1/2\mathrm{int}}) \\ (y - y_{1/2\mathrm{int}}) \\ (z - z_{1/2\mathrm{int}}) \end{bmatrix} \quad (2)$$

where (x, y, z) is the coordinate of the updated reference measurement point; $x_{1/2\mathrm{int}}$ = round(x), $y_{1/2\mathrm{int}}$ = round(y), and $z_{1/2\mathrm{int}}$ = round(z) are coordinates providing the location of the nearest half-integer voxel of coordinate point (x, y, z); the vector can be defined as the center point of the offset reference sub-volume. u, v, and w are three displacement components and u_x, u_y, u_z, v_x, v_y, v_z, w_x, w_y, and w_z are nine displacement gradient components.

In the conventional IC-GN algorithm, the gradients of the intensity within the reference sub-volume $\nabla f(f_x, f_y, f_z)$ are gradients under integer voxel conditions. Since the deformed volume image matrix is interpolated, the differential formula needs to be corrected as:

$$\nabla f = \left(\frac{\partial f(\mathbf{x}+\xi)}{\partial x} \quad \frac{\partial f(\mathbf{y}+\xi)}{\partial y} \quad \frac{\partial f(\mathbf{z}+\xi)}{\partial z} \right) \Big/ \alpha \quad (3)$$

where α is the interpolation coefficient.

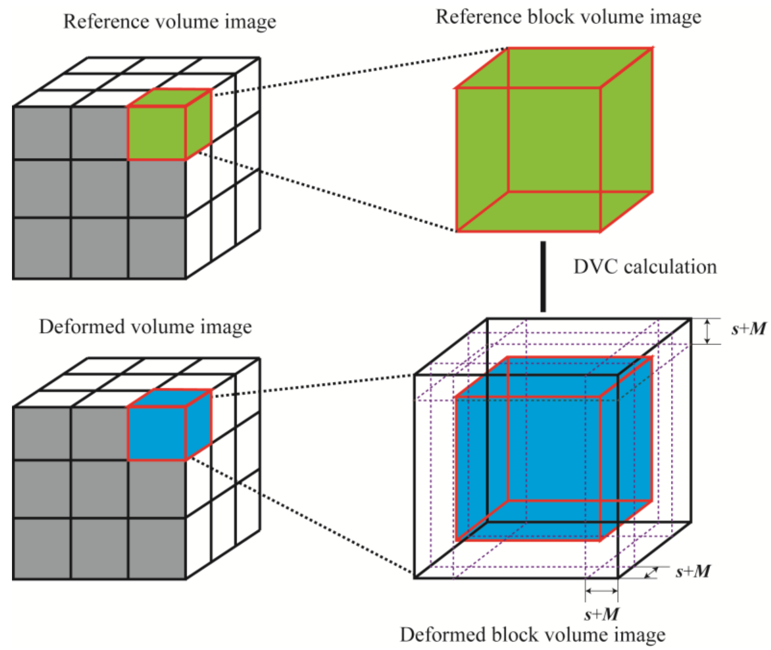

Fig. 3. Schematic of the block calculation method (s is the maximum displacement and M is sub-volume size).

2.2 Curve-fitting—small strain

In real DVC strain analysis, the strain error is difficult to control if the deformation is too large. Generally, the average strain level of the material is small (usually less than 5%); however, the local strain may be large (for example, the shear strain of some shear bands may exceed 20%). It is time-consuming to fully utilize the IC-GN algorithm in terms of calculating small strains. In the iterative process of the IC-GN algorithm, the calculation of the multiplication and inversion of the remaining matrices is still very large, even though the Hessian matrix only needs to be calculated once. In the DIC algorithm, the computational speed of the curve-fitting algorithm is seven times that of the IC-GN algorithm;[12,13] the computational speed difference between these two algorithms will be more disparate in the DVC algorithm. Therefore, the curve-fitting method is more suitable for calculating small deformation regions. Three algorithms, including the curve-fitting method, gradient-based method, and the Newton method, were compared in terms of calculation accuracy and stability.[12] The Newton method has the best calculation accuracy and stability; the gradient-based method is the second; the curve-fitting method is the worst (the accuracies and stabilities of the Newton method and IC-GN are almost the same[13]). The accuracy and stability of the curve-fitting method can barely meet the calculation requirements. In addition, the pre-interpolation calculation method described in Section 2.1 is also applied to the curve-fitting algorithm in order to improve the accuracy and stability.

First, the location of the extreme point of the zero-normalized cross-correlation (ZNCC) is calculated by the integer search algorithm; the ZNCC function is established at the extreme point. The ZNCC function can be set as $C(x,y,z)$ and the general curve-fitting equation is a ternary quadratic function:[14]

$$C_{ZNCC} = \frac{\sum_{\xi}\{[f(\mathbf{x}+\mathbf{W}(\xi;\Delta\mathbf{p}))-f_m]\cdot[g(\mathbf{x}+\mathbf{W}(\xi;\mathbf{p}))-g_m]\}}{\Delta f\cdot\Delta g} \tag{4}$$

$$C(x,y,z) = a_0 + a_1x + a_2y + a_3z + a_4xy + a_5xz + a_6yz + a_7x^2 + a_8y^2 + a_9z^2 \tag{5}$$

In some research, the least squares method is used to solve the equation parameters;[12,15] however, the least squares method involves complicated and time-consuming matrix operations. The explicit method is used for acceleration while the accuracy and stability of the existing explicit calculation method are insufficient.[14] Therefore, this method needs to be improved and solved using Eq. (12), which can be found in the appendix where detailed derivation processes are included.

3 Experimental verification using numerical tests

3.1 Accuracy of the proposed DVC method

In this work, a 100×100×100 voxel size referencing a 3D speckle pattern (R=4 voxels, s=12,000) was first generated, as shown in the inset of Fig. 4(a). Then, according to the Fourier shift theorem,[16] ten pure rigid body translation volume images were generated as the deformed volume images. Along the z direction, the displacements range from 0 to 1 voxel (0.0, 0.1, 0.2, 0.3, ..., 0.9, 1.0 voxel); the displacements of the x direction and y direction are zero. The random Gaussian noise with a mean value of zero and a variance of four was added to the previous eleven volume images. All DVC analyses were calculated by DVC software written using MATLAB 2018b language on a desktop computer (i7-6700 CPU 3.40 GHz and 8 GB RAM); the free GUI can be found at the following website: https://github.com/lichengshengHK/FastDVC.

The result of the IC-GN algorithm represents the existing incremental DVC algorithm result when $\alpha = 1$; this means that the incremental DVC algorithm proposed in reference[8] is a special case of the proposed method in this work. As shown in Figs. 4(a) and (b), for the existing incremental algorithm, the accuracy of the algorithm will be significantly reduced to be far from the accuracy of the conventional IC-GN algorithm when the sub-voxel displacement is in a certain range. Moreover, 1/2 sub-voxel interpolation is performed on the deformed volume image when $\alpha = 2$; the result of IC-GN calculation shows that the insufficiency of the incremental algorithm can be effectively improved. Particularly, the maximum mean bias error is reduced by 34% and the maximum random errors are reduced by 75% when the sub-voxel displacement is between 0.4 and 0.6 voxels. The improvement of the mean bias error and random error is very significant. According to the trend of the curves, the period and amplitude of the mean bias error curves of $\alpha = 2$ are about half of those of the mean bias error curves of $\alpha = 1$. Since the interpolation calculation is completed before the formal DVC calculation, the interpolation calculation time can be almost ignored; however, the improvement of the accuracy and stability of the algorithm is particularly remarkable. Furthermore, the accuracy of the DVC algorithm is very close to that of the traditional IC-GN algorithm when $\alpha = 2$. The specific comparison of algorithms can be found in Ref. 6.

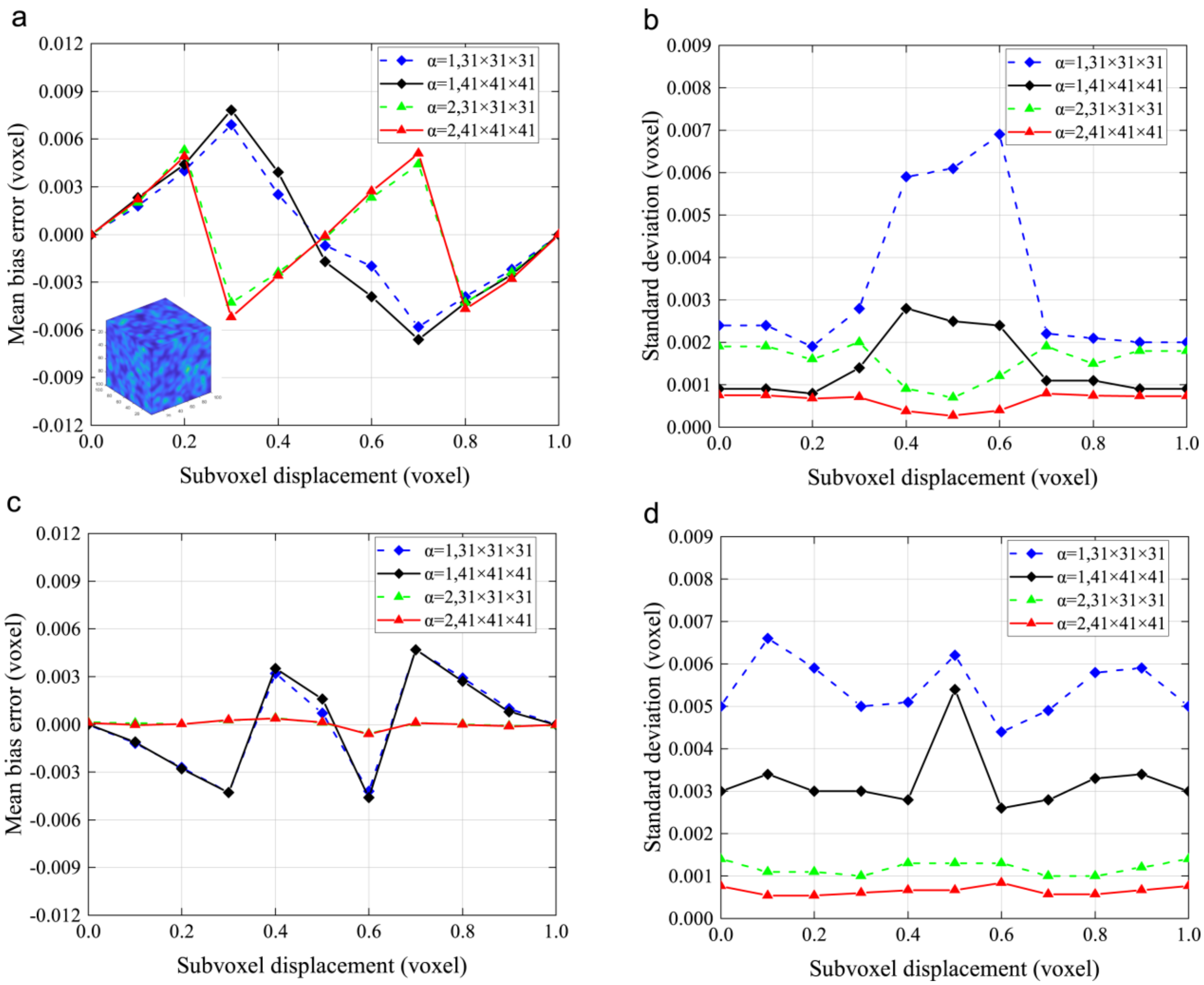

Fig. 4. Measured z displacements as a function of sub-voxel displacement estimated by different α and different sub-volume sizes: (a) mean bias error and (b) standard deviation error of the proposed DVC method of IC-GN method; (c) mean bias error and (d) standard deviation error of curve-fitting method.

As shown in Figs. 4(c) and (d), the mean bias error of the curve-fitting method is close to that of the IC-GN method when $\alpha = 1$; the maximum error is about 0.003 voxels. However, the difference between the random errors of these two algorithms approaches one order of magnitude. Therefore, it is unreasonable to use the curve-fitting method to estimate the sub-voxel displacement directly. The curve-fitting calculation is much more accurate compared to the existing IC-GN algorithm when the deformed volume is pre-interpolated by a 1/2 sub-voxel (α = 2). Not only can the mean bias error of sub-voxel displacement be reduced nearly ten times, but the random errors can also be well controlled, which is very close to the random errors of the IC-GN algorithm and fully meets the requirements of a real calculation. The pre-interpolation method can effectively improve the calculation accuracy and stability of the curve-fitting method while retaining the outstanding advantages of high computational efficiency and simple programming.

The interpolation coefficients are set as α = 1,2,3,4 and the window sub-matrix is set to the sub-volume size of 41×41×41 in order to verify the accuracy and stability of the algorithm under different interpolation coefficients α. Calculation results are shown in Fig. 5 and it can be seen that the IC-GN algorithm has better accuracy and stability. The mean bias error and standard deviation (SD) error of the IC-GN algorithm gradually decrease when the interpolation coefficient α increases from 1 to 3. However, the stability of the IC-GN algorithm deteriorates and mutations occur in some sub-voxel displacement when α = 4. In addition to memory consumption, the accuracy of the algorithm can be improved by appropriately increasing the interpolation coefficient α.

The accuracy and stability of the algorithm are improved when the interpolation coefficient α increases from one to two. However, the curve-fitting algorithm is less fortunate than the IC-GN algorithm when the interpolation coefficient α > 2; meanwhile, the mean bias error of the algorithm becomes very unstable. Moreover, the SD error increases by nearly seven times its initial value. In these cases, the curve-fitting algorithm cannot meet the calculation accuracy requirements. It can be illustrated from the above analysis that some interpolation errors could be easily caused if the interpolation coefficient is too large, affecting the accuracy and system stability of the DVC algorithm.

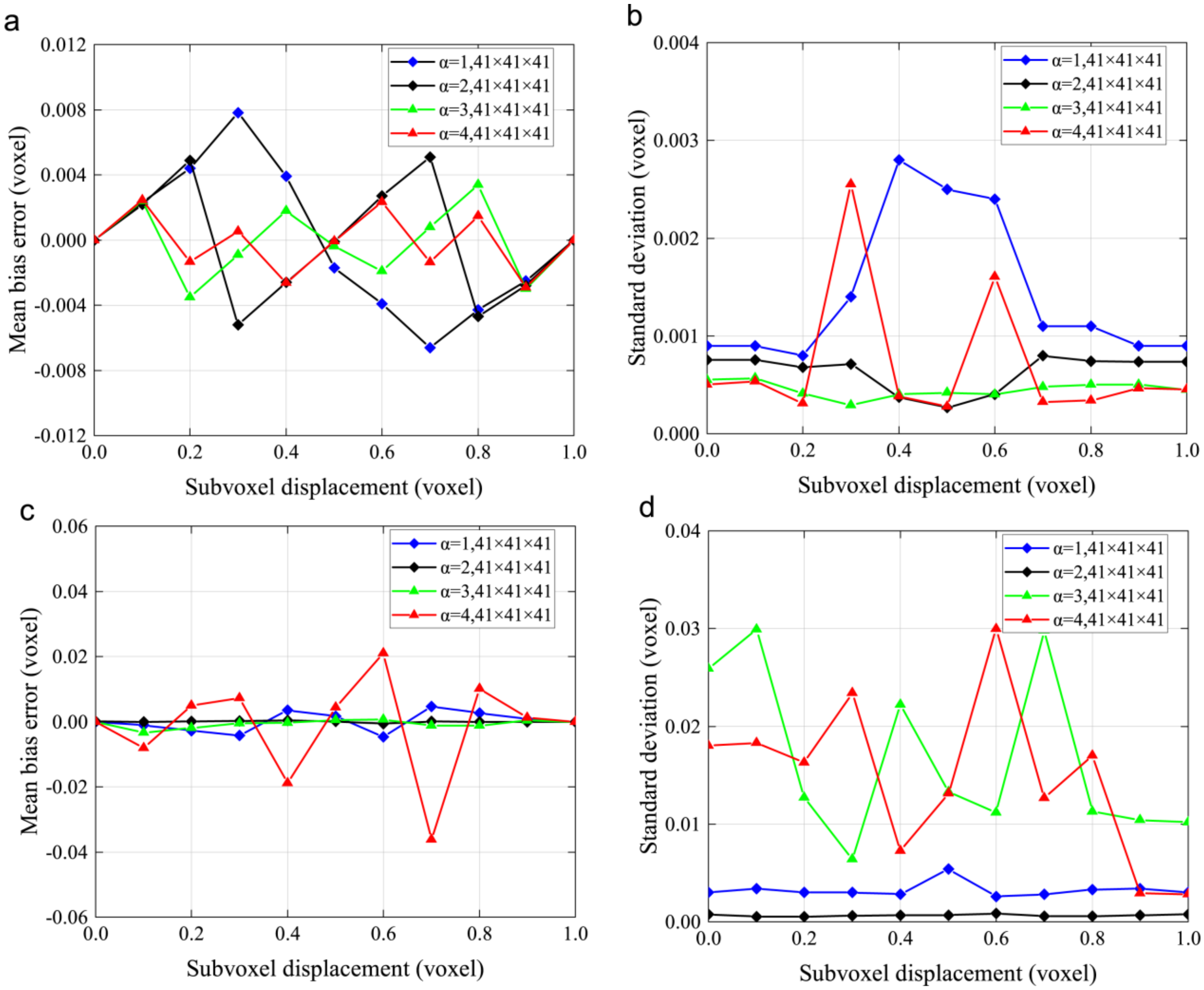

Fig. 5. Measured z displacements as a function of sub-voxel displacement estimated by different α: (a) mean bias error and (b) standard deviation error of the proposed DVC method of the IC-GN method; (c) mean bias error and (d) standard deviation error of the curve-fitting method.

Since the accuracy and stability of the algorithm could not be improved by the increase in the interpolation coefficient, it is necessary to find the optimal α. The memory requirement is increased by 27 times its initial value when the interpolation coefficient α = 3. The memory requirement is sharply increased to 64 times its initial value when the interpolation coefficient α = 4, seriously reducing the applicability of the algorithm. Considering the calculation accuracy and memory consumption of the algorithm, the interpolation coefficient α = 2 is the best choice. This not only ensures calculation accuracy but also does not occupy a massive amount of memory.

Moreover, as shown in Fig. 6, the curve-fitting algorithm has better accuracy than the IC-GN algorithm when α = 2. The SD of those two algorithms are similar; however, the mean bias error differs. The mean bias error of curve-fitting is 15 times less than that of IC-GN. Although curve-fitting can only deal with small strain deformation of materials, the improved curve-fitting not only has good accuracy but also has very high calculation efficiency. Therefore, it has a very high utilization value in small strain situations.

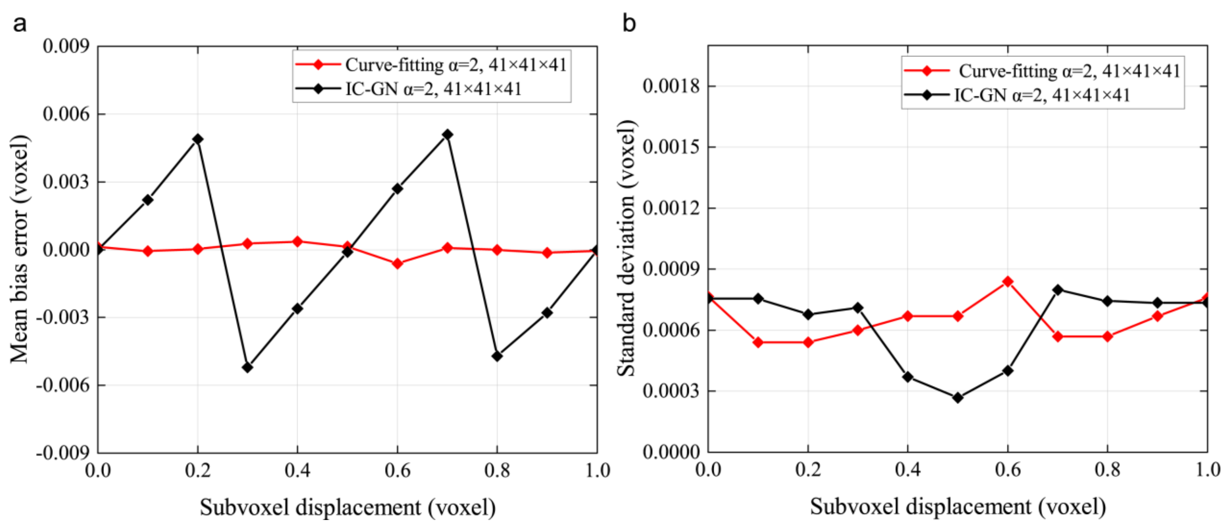

Fig. 6 Comparison of accuracy between the curve-fitting algorithm and IC-GN algorithm with α = 2, sub-volume size is 41×41×41: (a) mean bias error and (b) standard deviation error.

3.2. Computational efficiency of the proposed DVC method

The proposed algorithm has better accuracy and stability when the interpolation coefficient α = 2. In this section, the computational efficiencies of the two algorithms under different conditions are compared. Selecting α = 1 and 2, the computational speeds of the curve-fitting method and the IC-GN method are compared. The IC-GN algorithm has the same computational speed as existing incremental DVC algorithms when α = 1. Due to the use of different programming languages and computer configurations, the computational speed in this paper is slower than that in Ref. 8 (MATLAB programs are much slower than C++ in general). As shown in Fig. 7, the computational speed of the curve-fitting method can reach 757.38 points/s and the improved IC-GN algorithm can reach 237.35 points/s when α = 2 and sub-volume size is 41×41×41. The computational speed of the curve-fitting algorithm is 3.2 times that of the IC-GN algorithm. It can be seen that the curve-fitting algorithm is much faster than the IC-GN algorithm. The computational speed of the small deformation region in the material can be greatly improved and the displacement of the large deformation region can also be accurately estimated when calculating the strain field of a real material.

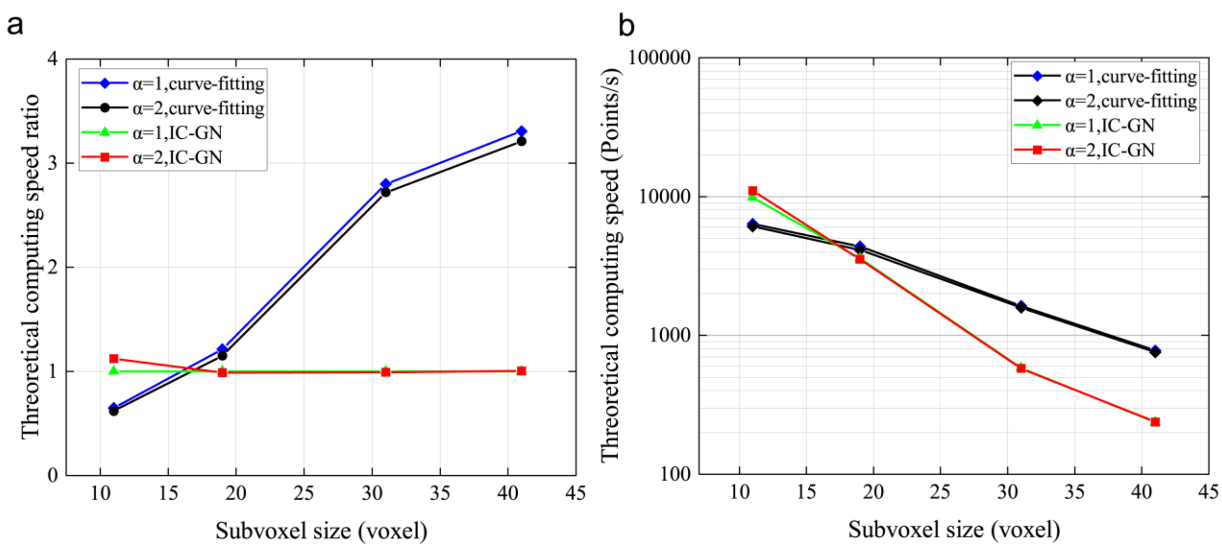

Fig. 7. Comparison of experimental computational speed of the improved IC-G methods to the improved curve-fitting method using various sub-volumes (the computation speed of the IC-GN algorithm with α = 1 is considered the standard)

4 Discussion and Conclusions

In this work, a pre-interpolation method is proposed that typically uses a 1/2 sub-voxel interpolation. It was only necessary to calculate the pre-interpolation once and the reference sub-volumes in the updated reference volume image automatically translated into the nearest half-integer voxel position. Therefore, the redundant sub-voxel interpolation calculation was avoided completely. Compared with the integer increment algorithm, the proposed method can improve the accuracy and retain high computational efficiency. Additionally, the curve-fitting algorithm was improved by the pre-interpolation method, whose accuracy and computational efficiency improved significantly. It was also found that if the interpolation coefficient larger than two, the error of the IC-GN algorithm and the curve-fitting algorithm increases; simultaneously, the memory requirement also increases significantly.

The simulation results show that the proposed improved DVC algorithm has better performance in accuracy, computational efficiency, and ease of implementation compared to the already existing DVC algorithm. In the MATLAB programming environment, the computational speed is increased by 1-3.2 times the original value, which can effectively improve the accuracy and efficiency of the DVC algorithm. Future studies will investigate how to use IC-GN and curve-fitting algorithms more effectively.

Appendix

This is the curve-fitting method

In this appendix, the steps of solving the curve-fitting Eq. (5) are illustrated in detail. First, for the convenience of writing, the 19 nodes in the cube lattice are marked as follows:

$$\begin{cases} C_1 = C(0,0,0) & C_{11} = C(-1,1,0) \\ C_2 = C(1,0,0) & C_{12} = C(1,0,1) \\ C_3 = C(-1,0,0) & C_{13} = C(-1,0,-1) \\ C_4 = C(0,1,0) & C_{14} = C(1,0,-1) \\ C_5 = C(0,-1,0) & C_{15} = C(-1,0,1) \\ C_6 = C(0,0,1) & C_{16} = C(0,1,1) \\ C_7 = C(0,0,-1) & C_{17} = C(0,-1,-1) \\ C_8 = C(1,1,0) & C_{18} = C(0,1,-1) \\ C_9 = C(-1,-1,0) & C_{19} = C(0,-1,1) \\ C_{10} = C(1,-1,0) & \end{cases} \tag{6}$$

instrumental variables:

$$\begin{cases} h_0 = C_1 \\ h_1 = (C_2 - C_3)/2 \\ h_3 = (C_4 - C_5)/2 \\ h_4 = (C_6 - C_7)/2 \\ h_5 = (C_8 + C_9 - C_{10} - C_{11})/4 \\ h_6 = (C_{16} + C_{17} - C_{18} - C_{19})/4 \\ h_7 = (C_2 + C_3)/2 - C_1 \\ h_8 = (C_4 + C_5)/2 - C_1 \\ h_9 = (C_6 + C_7)/2 - C_1 \end{cases} \tag{7}$$

$$\begin{cases} p_1 = (C_8 + C_{10} - C_{11} - C_9 + C_{12} + C_{14} - C_{15} - C_{13})/8 \\ p_2 = (C_8 + C_{11} - C_9 - C_{10} + C_{18} + C_{16} - C_{19} - C_{17})/8 \\ p_3 = (C_{15} + C_{12} - C_{13} - C_{14} + C_{16} + C_{19} - C_{18} - C_{17})/8 \end{cases} \tag{8}$$

$$\begin{cases} q_1 = (C_8 + C_{11} + C_9 + C_{10} + C_{15} + C_{12} + C_{13} + C_{14} - C_{18} - C_{16} - C_{19} - C_{17})/8 - h_0/2 \\ q_2 = (C_8 + C_{11} + C_9 + C_{10} - C_{15} - C_{12} - C_{13} - C_{14} + C_{18} + C_{16} + C_{19} + C_{17})/8 - h_0/2 \\ q_3 = (-C_8 - C_{11} - C_9 - C_{10} + C_{15} + C_{12} + C_{13} + C_{14} + C_{18} + C_{16} + C_{19} + C_{17})/8 - h_0/2 \end{cases} \tag{9}$$

According to the Eq. (6)~(9), the curve-fitting equation parameters can be obtained:

$$\begin{cases} a_1 = (h_1 + p_1)/2 \\ a_2 = (h_2 + p_2)/2 \\ a_3 = (h_3 + p_3)/2 \\ a_4 = h_4 \\ a_5 = h_5 \\ a_6 = h_6 \\ a_7 = (h_7 + q_1)/2 \\ a_8 = (h_8 + q_1)/2 \\ a_9 = (h_9 + q_1)/2 \end{cases} \tag{10}$$

the extreme points of the fitting function $C(x,y,z)$ should satisfy the following equations:

$$\begin{cases} \dfrac{\partial C(x,y,z)}{\partial x} = a_1 + a_4 y + a_5 z + 2a_7 x = 0 \\ \dfrac{\partial C(x,y,z)}{\partial y} = a_2 + a_4 x + a_6 z + 2a_8 y = 0 \\ \dfrac{\partial C(x,y,z)}{\partial z} = a_3 + a_5 x + a_6 y + 2a_9 z = 0 \end{cases} \tag{11}$$

solving the Eq. (11) and the sub-voxel displacement is given as:

$$\begin{cases} x = -\dfrac{a_1 \cdot F_1 + a_4 \cdot F_2 + a_5 \cdot F_3}{2a_7 \cdot F_1} \\ y = \dfrac{F_2}{F_1} \\ z = \dfrac{F_3}{F_1} \end{cases} \tag{12}$$

where

$$\begin{cases} F_1 = b_0 b_5 - b_2 b_3 \\ F_2 = b_1 b_5 - b_2 b_4 \\ F_3 = b_1 b_3 - b_0 b_4 \end{cases}, \quad \begin{cases} b_0 = a_4^2 - 4a_7 a_8, \quad b_3 = a_4 a_5 - 2a_6 a_7 \\ b_1 = 2a_2 a_7 - a_1 a_4, \; b_4 = 2a_3 a_7 - a_1 a_5 \\ b_2 = 2a_6 a_7 - a_4 a_5, b_5 = 4a_7 a_9 - a_5^2 \end{cases}.$$

References

1. B. Pan et al., "TOPICAL REVIEW: Two-dimensional digital image correlation for in-plane displacement and strain measurement: a review," Meas. Sci. Technol. 20(6), 152-154 (2009) [doi: 10.1088/0957-0233/20/6/062001].
2. B. K. Bay et al., "Digital volume correlation: Three-dimensional strain mapping using X-ray tomography," Experimental Mechanics 39(3), 217-226 (1999) [doi: 10.1007/BF02323555].
3. M. Mostafavi et al., "Quantifying yield behaviour in metals by X-ray nanotomography," Sci Rep 6(34346), (2016) [doi:10.1038/srep34346]
4. Y. Chen et al., "MICRO-CT BASED FINITE ELEMENT MODELS OF CANCELLOUS BONE PREDICT ACCURATELY DISPLACEMENT ONCE THE BOUNDARY CONDITION IS WELL REPLICATED: A VALIDATION STUDY," Journal of the Mechanical Behavior of Biomedical Materials 65(644-651 (2017) [doi:10.1016/j.jmbbm.2016.09.014].
5. A. Buljac et al., "Digital Volume Correlation: Review of Progress and Challenges," Experimental Mechanics 3), 1-48 (2018) [doi:10.1007/s11340-018-0390-7].
6. B. Pan et al., "An efficient and accurate 3D displacements tracking strategy for digital volume correlation," Optics Lasers in Engineering 58(4), 126-135 (2014) [doi:10.1016/j.optlaseng.2014.02.003].
7. E. Bar-Kochba et al., "A Fast Iterative Digital Volume Correlation Algorithm for Large Deformations," Experimental Mechanics 55(1), 261-274 (2015) [doi:10.1007/s11340-014-9874-2].
8. W. Bo, and P. Bing, "Incremental digital volume correlation method with nearest subvolume offset: An accurate and simple approach for large deformation measurement," Advances in Engineering Software 116(80-88 (2018) [doi:10.1016/j.advengsoft.2017.12.004].
9. B. Wang, and B. Pan, "Self-Adaptive Digital Volume Correlation for Unknown Deformation Fields," Experimental Mechanics 59(2), 149-162 (2019) [doi:10.1007/s11340-018-00455-2].

10. S. Baker, and I. Matthews, "Lucas-Kanade 20 years on: A unifying framework," International Journal of Computer Vision 56(3), 221-255 (2004) [doi:10.1023/b:visi.0000011205.11775.fd].

11. M. Gates, M. T. Heath, and J. Lambros, High-performance hybrid CPU and GPU parallel algorithm for digital volume correlation, Sage Publications, Inc. (2015) [doi:10.1177/1094342013518807].

12. P. Bing et al., "Performance of sub-pixel registration algorithms in digital image correlation," Measurement Science Technology 17(6), 1615 (2006) [doi:10.1088/0957-0233/17/6/045].

13. B. Pan, K. Li, and W. Tong, "Fast, Robust and Accurate Digital Image Correlation Calculation Without;Redundant Computations," Experimental Mechanics 53(7), 1277-1289 (2013) [doi:10.1007/s11340-013-9717-6].

14. M Wang et al., " Digital image correlation method for the analysis of 3-D internal displacement field in object," ACTA PHYSICA SINICA 55(10), 5135-5139 (2006) [doi:10.1016/S1872-1508(06)60029-6].

15. P. Bing et al., " Sub-pixel Registration Using Quadratic Surface Fitting in Digital Image Correlation," ACTA METROLOGICA SINICA (2004) [doi:10.3321/j.issn:1000-1158.2005.02.008].

16. H. W. Schreier, and M. A. Sutton, "Systematic errors in digital image correlation due to undermatched subset shape functions," Experimental Mechanics 42(3), 303-310 (2002) [doi:10.1007/bf02410987].

First Author is an assistant professor at the University of Optical Engineering. He received his BS and MS degrees in physics from the University of Optics in 1985 and 1987, respectively, and his PhD degree in optics from the Institute of Technology in 1991. He is the author of more than 50 journal papers and has written three book chapters. His current research interests include optical interconnects, holography, and optoelectronic systems. He is a member of SPIE.

Caption List

Fig. 1 Schematic illustration of the principle of the 3D IC-GN algorithm.

Fig. 2 Schematic illustration of the implementation of cubic spline interpolation with α = 2: (a) local interpolation unit comprised of 4×4×4 voxels; (b) interpolation block surrounded by 8 integer voxel points (blue) and 19 half-integer voxel points (green); and (c) schematic of the nearest sub-volume offset approach for incremental DVC.

Fig. 3 Schematic of the block calculation method (s is the maximum displacement and M is sub-volume size).

Fig. 4 Measured z displacements as a function of sub-voxel displacement estimated by different α and different sub-volume size: (a) mean bias error and (b) standard deviation error of the proposed DVC method of IC-GN method; (c) mean bias error and (d) standard deviation error of curve-fitting method.

Fig. 5 Measured z displacements as a function of sub-voxel displacement estimated by different α: (a) mean bias error and (b) standard deviation error of the proposed DVC method of the IC-GN method; (c) mean bias error and (d) standard deviation error of the curve-fitting method.

Fig. 6 Comparison of accuracy between the curve-fitting algorithm and IC-GN algorithm with α = 2, sub-volume size is 41×41×41: (a) mean bias error and (b) standard deviation error.

Fig. 7 Comparison of experimental computational speed of the improved IC-G methods to the improved curve-fitting method using various sub-volumes (the computation speed of the IC-GN algorithm with α = 1 is considered the standard)